Flows," *Flow Visualization III,* edited by W. J. Yang, Hemisphere, Washington DC, 1985, pp. 123-127.

[3]McGregor, I., "The Vapour-Screen Method of Flow Visualization," *Journal of Fluid Mechanics,* Vol. 11, Dec. 1961, pp. 481-511.

[4]Nelson, R. C., "The Use of Flow Visualization for Vortex Trajectory Mapping," *Flow Visualization III,* edited by W. J. Yang, Hemisphere, Washington DC, 1985.

[5]Brand, A. G., Komerath, N. M., McMahon, H. M., "Results from Laser Sheet Visualization of a Periodic Rotor Wake," AIAA Paper 88-0192, Jan. 1988.

[6]Brand, A. G., McMahon, H. M., Komerath, N. M., "Wind Tunnel Data From a Rotorwake/Airframe Interaction Study," School of Aerospace Engineering, Georgia Institute of Technology, Atlanta, GA. Contract No. DAAG29-82-K-0094, July 1986.

Thick Airfoil at Low Reynolds Number and High Incidence

S. Raghunathan,* J. R. Harrison,† and B. D. Hawkins†
The Queen's University of Belfast
Belfast, Northern Ireland, United Kingdom

Nomenclature

c = chord length
C_c = chordwise force coefficient, $= C_l \sin\alpha - C_d \cos\alpha$
C_d = drag coefficient, $= D/(\frac{1}{2}\rho V_\infty^2 c)$
C_l = lift coefficient, $= L/(\frac{1}{2}\rho V_\infty^2 c)$
C_p = pressure coefficient, $= (p - p_\infty)/(\frac{1}{2}\rho V_\infty^2)$
D = drag force
F_c = chordwise force
F_n = force normal to chord
p = static pressure on the airfoil
p_∞ = freestream static pressure
V_∞ = freestream velocity
x = chordwise coordinate
α = angle of incidence
ρ = density of air

Introduction

AIR turbines used for wind and wave energy conversion have rotors with airfoil blades that operate over a wide range of Reynolds numbers and airflow incidence. Aerodynamics data on airfoils at low Reynolds numbers are available for some airfoils up to stall angle and for a few airfoils beyond stall (see, for example, Refs. 1–6). The understanding of the performance of a thick symmetrical airfoil at low Reynolds numbers and over a range of incidence of 0–90 deg is of particular importance to a Wells self-rectifying air turbine used for wave energy conversion.[7,8] In a Wells turbine, the blades are set at a stagger angle of 90 deg. This Note presents some experimental data on an NACA 0021 airfoil at a blade chord Reynolds number of 2.6×10^5 and over a range of incidence of 0–90 deg. The results are compared with some of the data available on other airfoils and predictions by momentum theory.

Received Oct. 2, 1987; revision received Oct. 27, 1987.

*Reader, Aeronautical Engineering.
†Graduate Student.

Experiments

Isolated Airfoil

The experiments were conducted in a 0.84×1.145-m closed-circuit low-speed wind tunnel that had a contraction ratio of 3 and a turbulence level in the test section of 0.2%. The model was an NACA 0021 airfoil section of 100-mm chord and spanning the width of the test section. The model was made of three sections of equal span with pressure orifices on the centerline of the midsection. There were 13 pressure orifices each on the upper and lower surfaces, one at the leading edge, and one at the trailing edge. Pressure measurements were made by a Scanivalve with a Druck transducer linked to an RML 380Z computer. Tests were performed at a freestream velocity of $V = 38$ m/s, which corresponded to a blade chord Reynolds number of 2.6×10^5, and over a range of airflow incidences from 0–90 deg. Lift and drag values were calculated by integration of pressure distributions and were corrected for tunnel blockage effects. Oil-flow visualization studies were made for some selected test conditions.

Results and Discussion

The pressure distributions on the upper and lower surfaces of an NACA 0021 airfoil for the incidence range 0 deg $< \alpha <$ 20 deg are shown in Figs. 1 and 2, respectively. Figure 3 shows a comparison of the present data for C_l for an NACA 0021 with those measured by Jacobs and Sherman[2] and Muller and Janson.[5] The variations of C_l with incidence over the range of incidence 0 deg $< \alpha <$ 90 deg are shown in Fig. 4. In this figure, the data for an NACA 0021 airfoil is compared with those of NACA 0015 and 0012 airfoils from Ref. 3 and predictions by momentum theory.[4] The results for chordwise force coefficient C_c for several airfoils[3,6] are compared with the present results in Fig. 5. It should be noted that the present data for C_c does not include skin-friction drag.

The C_p distribution on the upper surface (Fig. 1) shows that the trailing-edge pressure diverges significantly at $\alpha = 13$ deg. As seen from the pressure distributions on the upper surface, there is a complete separation on the upper surface at the incidence of 13 deg. The C_p distribution on the upper surface continues to change with the increase in α after stall, but only gradually; for $\alpha > 26$ deg the C_p distributions on the upper sur-

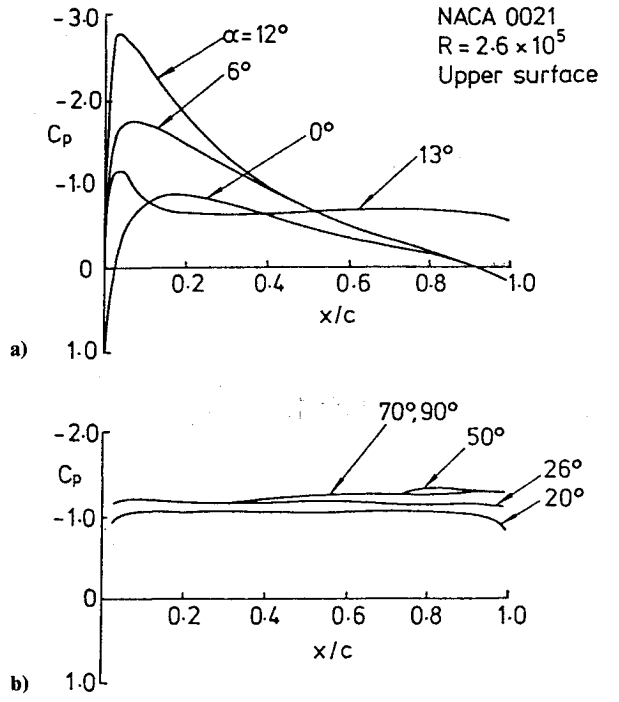

Fig. 1 Pressure distributions on the upper surface.

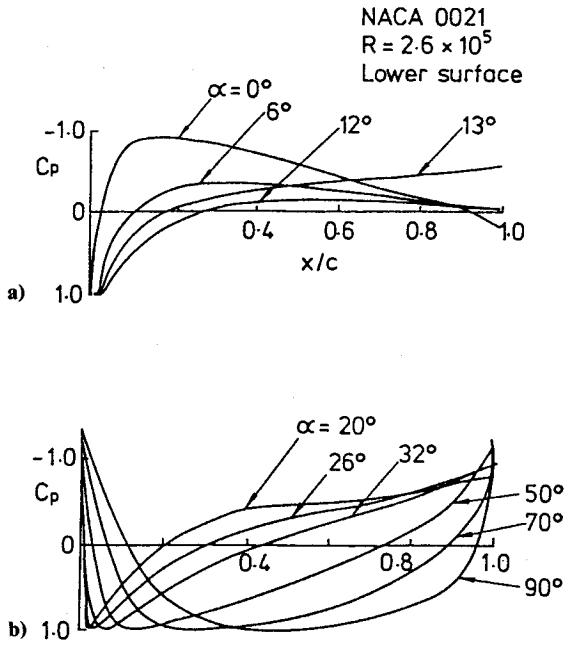

Fig. 2 Pressure distributions on the lower surface.

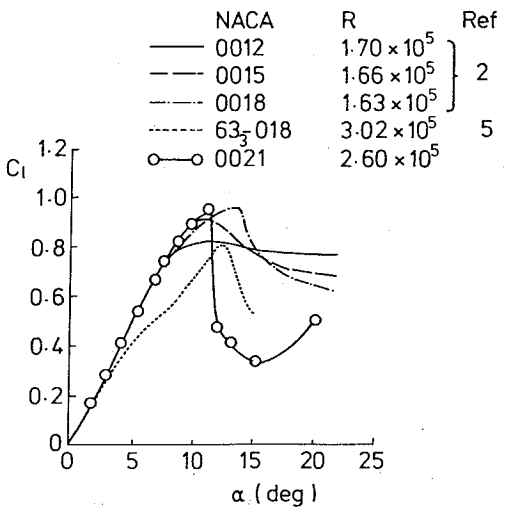

Fig. 3 Comparison of lift coefficients.

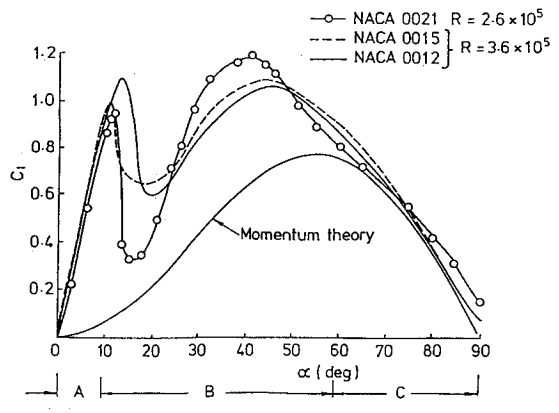

Fig. 4 Lift coefficients over a wide range of airflow incidences.

face are virtually unaffected by the variation in incidence. The C_p distribution on the lower surface (Fig. 2) changes with the increase in incidence over the entire incidence range of 0 deg $< \alpha <$ 90 deg. The extent of surface on the airfoil over

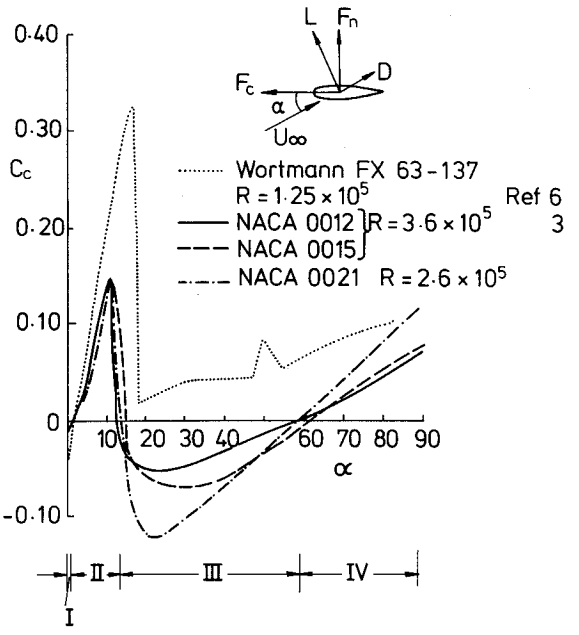

Fig. 5 Chordwise force coefficients.

which C_p is positive increases with the increase in incidence. The stagnation point ($C_p = 1$) moves rearward with the increase of α and is aft of the maximum thickness position for incidences close to 90 deg.

The aerodynamic force measurements on airfoils at low Reynolds numbers are critically dependent on the boundary-layer development on the airfoil surfaces. At low Reynolds numbers, the boundary-layer behavior is sensitive to Reynolds number, geometry, and aberration of the surface and tunnel environment such as freestream turbulence and noise.[6] Therefore, it is difficult to compare data for lift coefficients at different Reynolds numbers and measured in different test facilities. The present data for C_l for an NACA 0021 airfoil (Fig. 3) show an earlier stall when compared with the data for NACA 0012, NACA 0015, and NACA 0018 airfoils,[2] although the Reynolds number for the present data is higher.

The NACA 63_3-018 airfoil data[5] at somewhat even higher Reynolds number show a lower value of C_l maximum when compared with other airfoils. These differences could be attributed to the factors mentioned earlier. The general observations that can be made from these results are that at low Reynolds numbers ($1.60 \times 10^5 < R < 3 \times 10^5$) and for symmetric airfoil sections the maximum value of C_l, is between 0.8 and 1.0, the stall angle is between 10 and 15 deg and after stalling C_l decreases with incidence much more rapidly for thicker airfoils.

The C_l vs α curve over the range 0 deg $< \alpha <$ 90 deg (Fig. 4) can be roughly divided into three regions. The data on symmetric airfoils show that, in the incidence range 0 deg $< \alpha <$ 15 deg (region A), the lift produced is primarily by circulation. In the poststall region, where there is a second peak (region B), the lift produced is due to both momentum and circulation; for $\alpha >$ 50 deg (region C), the lift produced is primarily due to momentum. At $\alpha +$ 90 deg, the lift due to momentum is zero, but still there is a small positive lift produced due to circulation. This also can be observed from the pressure distributions (Figs. 1 and 2). In region C, the lift curve has almost the same slope as the momentum curve for a flat plate. In this region, the increase in lift with thickness ratio is due to a greater part of the boundary layer being attached around the leading edge and the consequent suction.

The C_c vs α curve (Fig. 5) for an airfoil can be divided into four regions. In region I, (0 deg $< \alpha <$ 3 deg), the values of C_c are negative due to the predominant effect of C_d in chordwise direction. In region II, which is the operation regime for air

turbines, the value of C_c is positive due to a significant component of lift that increases with α in the chordwise direction. For symmetrical airfoils, the values of C_c are negative in the poststall region III. The range of incidence for which the values of C_c are negative in this region increases with the increase in the thickness ratio of the airfoil. In region IV the values of C_c are positive again. In this region, the chordwise componenets of aerodynamic forces are dominated by the suction around the leading edge. The Wortmann FX63-137 airfoil data[6] show much larger values of C_c, which are positive in regions II, III, and IV. The C_c vs α curve for a symmetrical airfoil has a direct implication in the design of a Wells air turbine for self-starting characteristics.[7,8] When such as turbine starts from rest, there is sufficient torque to start the turbine rotating due to the fact that at $\alpha = 90$ deg, C_c is positive. As the turbine speed increases, α decreases. In order to move into the operational regime (region II), the turbine has to go through a region of negative torques (region III), which results in a turbine speed much lower than the operational speed. This phenomenon, known as crawling,[8] can be eliminated by increasing turbine solidity, which effectively results in a positive value of C_c in region III.

References

[1]Jacobs, E. N. and Abbot, I. H., "Aerofoil Section Data Obtained in the NACA Variable Density Tunnel," NACA TR 669, 1939.

[2]Jacobs, E. N. and Sherman, A., "Airfoil Section Characteristics Affected by Variation of Reynolds Number," NACA Rept. 586, 1937.

[3]Blackwell, B. F. and Sheldahl, R. E., "Aerodynamic Characteristics of Four Symmetrical Aerofoil Sections Through 180 deg Angle of Attack at Low Reynolds Number," Sandia Labs., Albuquerque, NM, Rept. 87115, 1976.

[4]Beans, E. W. and Jakubowski, G. S., "Method for Estimating the Aerodynamic Coefficients fo Wind Turbine Blades at High Angle of Attack," *AIAA Journal*, Vol. 7, June 1983, pp. 747–749.

[5]Muller, T. J. and Jansen, B. J., "Aerodynamic Measurements at Low Reynolds Numbers," AIAA Paper 82-0598, 1982.

[6]Muller, T. J., "Low Reynolds Number Vehicles," AGARD-AG-288, 1985, pp. 1–69.

[7]Raghunathan, S. and Tan, C. P., "Performance of the Wells Turbine at Starting," *Journal of Energy*, Vol. 6, 1982, pp. 430–431.

[8]Raghunathan, S. and Tan, C. P., "The Aerodynamics of Wells Turbine," *Journal of Energy*, Vol. 7, 1983, pp. 226–230.

Technical Comment

Comment on "Residual Stresses in 2024-T81 Aluminum Using Caustics and Moiré Interferometry"

Michael A. Landy*
Fatigue Technology, Inc.
Seattle, Washington

In Ref. 1, Leftheris and Schwarz discuss, among other topics, use of the split-sleeve cold-working process to produce residual strains in 2024-T81 aluminum. The widely used process, unexplained in the Note, involves the creation of residual compressive stresses by drawing an oversized mandrel through a hole using a prelubricated stainless steel split sleeve. The sleeve protects the hole wall from damage, insures that the axial motion of the mandrel is translated efficiently into force in the radial direction, and minimizes the force required to accomplish the operation. Typically, fatigue or crack-growth life improvements of 3:1, minimum, have been reported (Refs. 2–20, and others).

Leftheris and Schwarz split-sleeve cold-worked holes in 4 in. × 4 in. × 0.125 in. 2024-T81 plates, and then used moire interferometry to show the distribution of residual strains (Figs. 4 and 5, Ref. 1). They note in the text that at the location where the split in the sleeve was located, the residual tangential strains are "very low." Figures 4 and 5, however, show the residual tangential strain in the location at the sleeve-split to be the highest of any circumferential location. This is shown for both the specimen cold-worked with the sleeve-split aligned with the rolling direction L and the specimen expanded with the sleeve-split aligned 90 deg to the rolling direction L-T. The lowest residual tangential strain is shown at the location corresponding to the side of the hole opposite from the split.

Received Sept. 30, 1987; revision received Nov. 4, 1987.

*Engineering Manager. Member AIAA.

Based on the above observations, Leftheris and Schwarz conclude that

1) There is "an area sector spreading radially out from the sleeve seam, where the strains are near zero after cold work," and

2) "If a crack grows where the sleeve seam is positioned, fatigue enhancement may not occur from the cold work process."

These conclusions are unsubstantiated and contradictory to in-service experience and to the results of many other comprehensive fatigue and crack-growth investigations (Refs. 2–20) of split-sleeve cold-worked holes in various aluminums, titaniums, and steels under constant amplitude and broadband spectrum loading conditions.

Leftheris and Schwarz's data do show that for the specimen geometry tested, higher tangential residual strains were associated with longer crack-growth lives. Their contention, however, that zero residual strain is associated with no life improvement is misleading. Residual compressive *stresses* that, in general, determine life improvement associated with a cold-working process (assuming some geometry, load spectrum, etc.) may exist with positive, negative, or zero residual strains. Alternatively, high positive residual strains may exist in a situation where no compressive residual stresses exist (i.e., no life improvement): A part that yields completely during the cold-working process.

In general, investigators performing cyclic tests cold-work the specimen holes with the sleeve-split at 90 deg to the direction of applied loading. If, as Leftheris and Schwarz contend, fatigue enhancement may not occur in that area due to residual strains being near zero, how do they explain that most failures initiate and grow from the area of the hole opposite the split? The fact that failures do occur away from the split is substantiated by Leftheris and Schwarz's empirical data. As noted above, those data (Figs. 4 and 5) show the tangential residual strain to be the lowest at the so-called 270 deg position, corresponding to the area of the hole opposite the split. Leftheris and Schwarz neglected to report the failure location with respect to the sleeve-split in the tests they performed on crack growth of cold-worked holes.

In fact, the effectiveness of split-sleeve cold-working in the area near the split is simply no longer in doubt. Many investigators of the process have focused on it, concluding that the split does not affect the fatigue enhancement performance